A preventive control model for static voltage stability and thermal stability based on power transfer capabilities of weak branches

Wei Yan[1], Xiuqiong Hu[1], Juan Yu[1] and Wenyuan Li[1,2]
(1)The State Key Laboratory of Power Transmission Equipment & System Security and New Technology
Chongqing University
Chongqing
China
cquyanwei@cqu.edu.cn
huxiuqiongdu@163.com
dianlixi@ cqu.edu.cn
(2)British Columbia Transmission Corporation
Suite 1100, Four Bentall Center, 1055 Dunsmuir Street
Vancouver, BC, V7X 1V5
Canada
wen.yuan.li@bctc.com

Abstract: - A preventive control model for static voltage stability and thermal stability is presented using the apparent power constraints on weak branches as both static voltage stability constraints and thermal stability constraints. Firstly, a localized line-based voltage stability index is selected to determine the weak branches as well as their power transfer capabilities and the critical contingencies. A static security analysis method, which is based on PQ decouple method, is adopted to obtain the quadratic apparent power expressions of weak branches following each critical contingency. Then, the apparent power constraints on weak branches are established combining the power transfer capabilities and the apparent power expressions of weak branches. The proposed preventive control model has a quadratic form and can be solved by the predictor-corrector primal dual interior method. The simulation results for three IEEE test systems demonstrate the correctness and effectiveness of the proposed preventive control model.

Key-Words: - Preventive control, Static voltage stability, Thermal stability, Weak branch, Apparent power constraint, Quadratic optimal model

1 Introduction

In large-scale power grids with long distance transmission and high load level, the apparent powers on stressed weak branches may exceed their transfer capabilities in case of stressed load and/or component outage [1-3]. Consequently, static voltage instability and/or thermal instability possibly occur and eventually result in loss of load and even a collapse of power system. For example, in the August 14, 2003 blackout in North America, as a result of stressed load and several transmission line outages, the cascading thermal instability and voltage instability happened and resulted in the loss of 61.8 GW loads [4]. It is extremely important to use effective preventive control to improve the pre-contingency operating state of power system to guarantee the static voltage stability and thermal stability in various contingency and stressed load conditions.

The preventive control for static voltage stability and thermal stability is usually formulated using the optimal power flow (OPF) models [5-15]. References [5-13] proposed the linearized optimization models for preventive control in which the static voltage stability constraints and the thermal stability constraints were respectively expressed by the linear sensitivity of static voltage stability index and apparent power or current on transmission lines with respect to control variables. Unfortunately, the power system is a nonlinear system and the nonlinear characteristic is predominant when it is unstable or close to instability. A linearized model has limitations [16]. Reference [14] presented a nonlinear model for preventive control in which the static voltage stability constraints were expressed by power flow

equations with load parameter in normal operating and stressed load condition, whereas the thermal stability constraints were expressed by transfer current constraints. This control model can reflect the nonlinear characteristic of power system. Based on Reference [14], Reference [15] introduced multi-contingency conditions in a similar preventive control model for static voltage stability and thermal stability. However, when a power system is very large or a large number of critical contingencies must be considered, the number of static voltage stability and thermal stability constraints is extremely large and the preventive control model becomes very complicated. This results in difficulties in solving the model and even no feasible solution for the preventive control [17].

In real world, the static voltage instability and/or thermal instability generally originate from one or several weak branches whose apparent powers exceed their power transfer capabilities. If the static voltage stability and thermal stability constraints can be all expressed by the apparent power constraints on weak branches, the preventive control model will be greatly simplified. In order to achieve this goal, determining weak branches causing the static voltage stability problem is a crucial step. There are several localized line-based voltage stability indices which can identify weak branches [18-20]. Particularly, the voltage stability indices presented in References [19] and [20] can be used to estimate the power transfer capabilities of weak branches. And the localized line-based voltage stability index, which is called the Extended Line Stability Index (ELSI) in Reference [20], has considered the impact of external system beyond a line and can more precisely recognize weak branches and their transfer capabilities corresponding to the voltage collapse point.

Based on the concept above, this paper presents a preventive control optimal model using the apparent power constraints on weak branches as both static voltage stability and thermal stability constraints. ELSI and thermal limit of branches are used to determine critical contingencies as well as corresponding weak branches and their power transfer capabilities. A static security analysis based on PQ decoupled method is used to obtain the quadratic expressions for apparent powers of weak branches in each critical contingency, which leads to a quadratic preventive control model. It has been proved that a quadratic optimal model is very efficient in computations when the predictor-corrector primal dual interior point method (PCPDIPM) is used [21].

The rest of the paper is organized as follows. The formulation of the quadratic optimal model for preventive control is presented in Section 2. The simulation results are provided in Section 3, followed by conclusions in Section 4.

2 Formulation of Quadratic Optimal Model for Preventive Control

In this section, the static voltage stability and thermal stability constraints are established and the quadratic optimal model for preventive control is built. In the proposed preventive control, N-1 contingencies of branch outages are considered. Note that the normal operating state is treated as a special case of contingency condition in the mathematical expression.

2.1 Establishment of static voltage stability and thermal stability constraints

2.1.1 Determination of critical contingencies as well as corresponding weak branches and their transfer capabilities using ELSI and thermal limit of branches

The ELSI is calculated by Equation (1).

$$ELSI = \frac{E_k^2}{2[R_{kj}P_{ij} + X_{kj}Q_{ij}^* + \sqrt{(R_{ij}^2 + X_{ij}^2)(P_{ij}^2 + (Q_{ij}^*)^2)}]} \quad (1)$$

where R_{kj}+jX_{kj} is the equivalent line impedance of a line in which the effect of equivalent voltage source outside the two buses of the line has been incorporated; P_{ij}+jQ^*_{ij} is line complex power flow with the charging reactive power excluded at the receiving bus j; and E_k is the voltage of the equivalent voltage source outside the two buses of the line; the formulas of calculating E_k , R_{kj} , X_{kj} using localized information (line impedance and voltages at the two ends of a line) are derived in Reference [20].

The ELSI can be also used to calculate the power transfer capability of each branch (permissible MVA flow) by Equation (2).

$$S_{ij\max} = ELSI_{ij} \times S_{ij} \quad (2)$$

where $S_{ij\max}$, S_{ij} and $ELSI_{ij}$ respectively represent the power transfer capability, actual apparent power and ELSI of branch ij.

Reference [20] proved that the ELSI of each branch must be larger than 1.0 or equal to 1.0 for guaranteeing the static voltage stability of a power system. The larger the ELSI is, the farther the power system is from its voltage instability. In operation practice of utilities, operators do not allow their system to be operated very near the critical point of

voltage collapse and a secure margin must be applied. This corresponds to a threshold value of ELSI which is little bit larger than 1.0. The threshold is denoted by α in the proposed preventive control. The difference between α and 1.0 reflects the desired margin of static voltage stability, which can be determined by individual power companies.

The Equation (1) indicates that the only localized information is needed to calculate the ELSI. In real time application, the localized information is directly obtained from Phasor Measurement Units (PMU). In the off-line application of identifying weak branches in the preventive control, power flows are solved to provide the information required for calculating the ELSI of each potential weak branch in various contingency conditions. For a solvable case, the power flow can be directly calculated. However, for an unsolvable case, the ELSI or any other line-based voltage stability index cannot be calculated to identify system voltage instability and weak branches. Then, a minimizing load shedding model similar to that given in Reference [22] is used to restore solvability of power flow.

Based on the power flow solution, the ELSI and actual apparent power of each operating branch are calculated. For the contingency state of branch *kl* in outage, if the ELSI of any branch *ij* is smaller than α or the actual apparent power of branch *ij* is larger than its thermal limit, the contingency of branch *kl* in outage is determined to be a critical contingency, and branch *ij* is determined to be a weak branch whose permissible power transfer capability $S_{ij\_weak\max}$ can be expressed using the ELSI by Equation (3).

$$S_{ij\_weak\max} = \min\left\{ ELSI_{ij\_weak} \times S_{ij\_weak} \Big/ \alpha , S_{ijthl\max} \right\} \quad (3)$$

where S_{ij_weak} and $ELSI_{ij\_weak}$ respectively represent the actual apparent power and ELSI of branch *ij* in the contingency state of branch *kl* in outage, and $S_{ijthl\max}$ represents the thermal limit of branch *ij*.

It should be pointed out that the ELSI is not a unique index to represent such a permissible transfer capability. Conceptually, as long as a method can provide this power transfer capability of individual branches, Equation (3) can be used in the proposed model. The advantage of using the ELSI is that it can be quickly and easily calculated for individual branches from a regular power flow (solvable case) or a simple optimal power flow (unsolvable case) following a contingency. Also, the ELSI has considered the impacts of external system beyond a line.

2.1.2 Quadratic expression for apparent powers of weak branches in critical contingencies

In the critical contingency of branch *kl* in outage, the apparent power of weak branch *ij* can be calculated by Equations (4)-(6).

$$P_{ij1} = P_{ij0}(e,f) + \Delta P_{ij}(e,f) \quad (4)$$

$$Q_{ij1} = Q_{ij0}(e,f) + \Delta Q_{ij}(e,f) \quad (5)$$

$$S_{ij1}^2 = P_{ij1}^2 + Q_{ij1}^2 \quad (6)$$

where, S_{ij1}, $P_{ij1}$and Q_{ij1}respectively represent the apparent power, active power and reactive power of weak branch *ij* in the contingency of branch *kl* in outage; $P_{ij0}(e,f)$ and $Q_{ij0}(e,f)$, which are the quadratic functions of the real parts *e* and imaginary parts *f* of bus voltages in rectangular form[21], respectively represent the active power and the reactive power of branch *ij* in the normal operating condition;$\Delta P_{ij}(e, f)$and$\Delta Q_{ij}(e, f)$ respectively represent the active power increment and reactive power increment of weak branch *ij* in the contingency condition. Using the static security analysis based on the PQ decoupled method [23],$\Delta P_{ij}(e, f)$and$\Delta Q_{ij}(e, f)$ can be expressed by Equations (7) and (8), which are derived in Appendix .

$$\Delta P_{ij}(e,f) = [(S_{jk}^{'} - S_{ik}^{'})a_{11} + (S_{jl}^{'} - S_{il}^{'})a_{21}]b_{ij}P_{kl0}(e,f) + [(S_{jk}^{'} - S_{ik}^{'})a_{12} + (S_{jl}^{'} - S_{il}^{'})a_{22}]b_{ij}P_{lk0}(e,f) \quad (7)$$

$$\Delta Q_{ij}(e,f) = [(S_{jk}^{'}c_{11} + S_{jl}^{'}c_{21})b_{ij} - (S_{ik}^{'}c_{11} + S_{il}^{'}c_{21})(b_{ij} + 2b_{t0})]Q_{kl0}(e,f) + [(S_{jk}^{'}c_{12} + S_{jl}^{'}c_{22})b_{ij} - (S_{ik}^{'}c_{12} + S_{il}^{'}c_{22})(b_{ij} + 2b_{t0})]Q_{lk0}(e,f) \quad (8)$$

where, $S_{ik}^{'}$ and $S_{ik}^{''}$ respectively represent the *i*th row and *k*th column element of matrix $S^{'}$ and $S^{''}$; a_{11}, a_{12}, a_{21}, a_{22} and c_{11}, c_{12}, c_{21}, c_{22}, whose values can be obtained from Equations (A.3) and (A.4) in Appendix, are constants;$P_{kl0}(e, f)$ and $Q_{kl0}(e, f)$, $P_{lk0}(e, f)$ and $Q_{lk0}(e, f)$,which are the quadratic functions of *e* and *f*, respectively represent the active power and reactive power flowing from bus *k* to bus *l* , and the active power and reactive power flowing from bus *l* to bus *k* in the normal operating condition. It can be seen that$\Delta P_{ij}(e, f)$and$\Delta Q_{ij}(e, f)$ are also the quadratic functions of *e* and *f*.

2.1.3 Static voltage stability and thermal stability constraints

By combining the power transfer capability $S_{ij\_weak\max}$ given in Equation (3) and the apparent power expression of weak branch *ij*, the apparent power constraint on weak branch *ij* can be established by Equation (9).

$$S_{ij1}^2 = P_{ij1}^2 + Q_{ij1}^2 \le S_{ij\_weak\max}^2 \quad (9)$$

As long as there is one branch whose apparent

power exceeds its power transfer capability in a contingency, the static voltage stability violation and/or thermal stability violation will occur. Therefore, Equations (4), (5) and (9), which are the apparent power constraints on weak branches, can be used as the combined static voltage stability and thermal stability constraints.

Actually, there are only a few weak branches resulting in static voltage instability and/or thermal instability in a power system. In other words, the number of the combined static voltage stability and thermal stability constraints expressed by Equations (4), (5) and (9) is small. In this way, the proposed preventive control model for static voltage stability and thermal stability becomes a small scale optimization problem.

2.2 Proposed quadratic optimal model for preventive control

Using the static voltage stability and thermal stability constraints expressed by Equations (4), (5) and (9), the proposed preventive control model can be formulated by Equations (10)-(24).

In the proposed preventive control model, the objective is to minimize the load-shedding and the network active power loss. The unknown controllable variables to be optimized include the active power outputs P_G of generators, reactive power outputs Q_G of generators, reactive power injections Q_C of shunt capacitors, reactive power injections Q_R of shunt reactors, LTC (loading tap changers) turn ratios k and active load curtailments C. The unknown state variables to be optimized include the real parts e and imaginary parts f of bus voltages. The active powers P_{ij1} and reactive powers $Q_{ij1}$of weak branches in the corresponding critical contingencies are also considered as state variables to be optimized.

$$\min \quad \sum_{i\in N_B} P_{Gi} - \sum_{i\in N_B}(P_{Di}-C_i) + \sum_{i\in N_B} w_i C_i \quad (10)$$

s.t.

$$P_{Gi} - \sum_{ij\in S_{Li}} P_{Lij}(e,f) - (P_{Di}-C_i) - \sum_{ij\in S_{Ti}} P_{Tij}(e,f) = 0 \qquad i=1,...,N_B \quad (11)$$

$$Q_{Gi} + Q_{Ci} - \sum_{ij\in S_{Li}} Q_{Lij}(e,f) - \sum_{ij\in S_{Ti}} Q_{Tij}(e,f) - (Q_{Di} - C_i Q_{Di}/P_{Di}) + Q_{Ri} = 0 \qquad i=1,...,N_B \quad (12)$$

$$e_i f_m - e_m f_i = 0 \qquad t=1,...,N_T \quad (13)$$

$$e_i - k_t e_m = 0 \qquad t=1,...,N_T \quad (14)$$

$$U_{i\min}^2 \le e_i^2 + f_i^2 \le U_{i\max}^2 \qquad i=1,...,N_B \quad (15)$$

$$k_{t\min} \le k_t \le k_{t\max} \qquad t=1,...,N_T \quad (16)$$

$$P_{Gi\min} \le P_{Gi} \le P_{Gi\max} \qquad i=1,...,N_G \quad (17)$$

$$Q_{Gi\min} \le Q_{Gi} \le Q_{Gi\max} \qquad i=1,...,N_G \quad (18)$$

$$Q_{Ci\min} \le Q_{Ci} \le Q_{Ci\max} \qquad i=1,...,N_C \quad (19)$$

$$Q_{Ri\min} \le Q_{Ri} \le Q_{Ri\max} \qquad i=1,...,N_R \quad (20)$$

$$0 \le C_i \le P_{Di} \qquad i=1,...,N_B \quad (21)$$

$$P_{ij1} = P_{ij0}(e,f) + \Delta P_{ij}(e,f) \qquad ij \in S_{L\_weak} \quad (22)$$

$$Q_{ij1} = Q_{ij0}(e,f) + \Delta Q_{ij}(e,f) \qquad ij \in S_{L\_weak} \quad (23)$$

$$P_{ij1}^2 + Q_{ij1}^2 \le S_{ij\_weak\max}^2 \qquad ij \in S_{L\_weak} \quad (24)$$

In Equations (11) and (12), P_{Lij} (e, f), Q_{Lij} (e, f), and P_{Tij} (e, f), Q_{Tij} (e, f), which respectively represent the active and reactive powers on line branch or unload tap changer branch, are the quadratic functions of e and f [21]. The reactive power load curtailment at bus i is assumed to be proportional to C_i with a constant power factor, which is shown in Equation (12). Equations (13) and (14) represent the voltage conversion relation of LTC branches [21]. Equations (22)-(24), which are the same to Equations (4), (5) and (9), are the quadratic functions of optimal variables. w_i represents the weighting factor reflecting the importance of load at bus i; the magnitudes of the weighting factors only need to be selected in a relative sense. (Note that every weighting factor is set to be 100 in the given examples in Section 3, which indicates equal importance for loads at each bus.)

The proposed preventive control optimal model has the following three features:

- The model can absolutely reflect the nonlinear characteristics of power system since the nonlinear equality constraints for power flow and the quadratic constraints for the static voltage stability and thermal stability are accurately expressed by the nonlinear functions of variables. Therefore, it can overcome the limitations in linearized optimization models.
- The number of weak branches causing static voltage stability and thermal limit violation is always small in an actual power system. Using the apparent power constraints on weak branches to represent the static voltage stability and thermal stability constraints in the model has greatly reduced the size of the preventive control problem to be solved.
- The model is in a purely quadratic form because Equations (10)-(24) are either linear or quadratic functions of optimal variables. When the interior point method is used to solve the model, the Hessian matrix is calculated only once in the entire optimization process. This feature, together with the characteristic of the small

number of constraints, makes the model computationally efficient.

2.3 General Flow Chart of the proposed Preventive Control

The general flow chart for the proposed preventive control is shown in Fig.1, in which *i* denotes the *i*th contingency, and *k* denotes the iteration index of the preventive control.

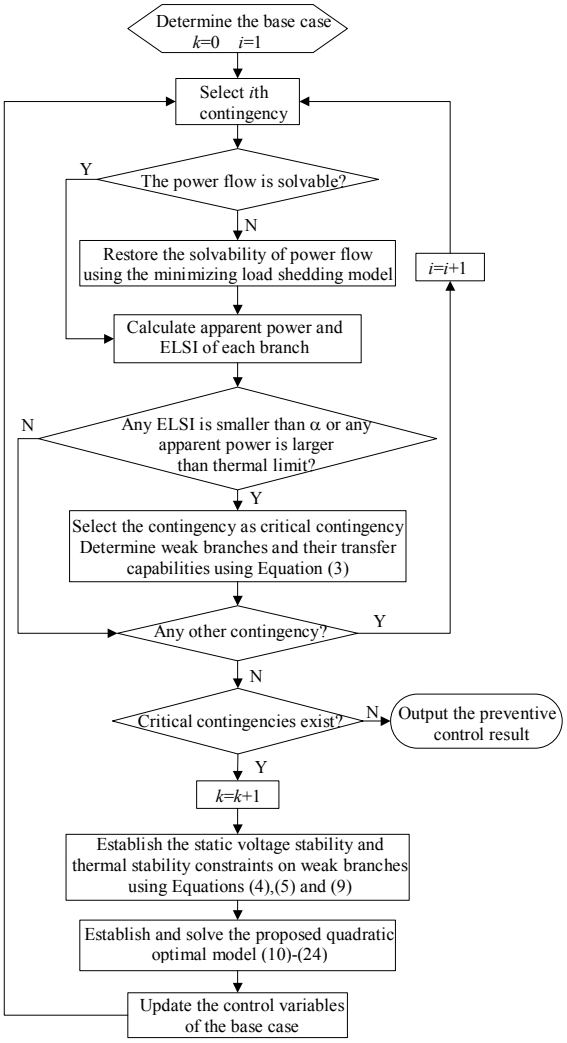

Fig.1. General flow chart of the proposed preventive control

In the general flow chart, there are two points should be noted:

- There are two reasons for using the iteration index *k* of the preventive control. One hand, the static security analysis based on PQ decoupled method possibly results in deviation of active power and reactive power in Equations (7) and (8) from the actual active power and reactive power when the system is close to instability point; the other hand, the proposed preventive control result based on only the apparent power constraints on several weak branches can't ensure there are no static voltage stability violations and/or thermal stability violations on other lines. Therefore, the iteration index *k* must be used to check whether the preventive control result in iteration can absolutely guarantee the system satisfies the desired static voltage stability margin and thermal stability in various contingency conditions.
- Resorting the solvability of power flow, which generally uses the minimizing load shedding model, is usually considered as a corrective control. However, the corrective control isn't explicitly addressed in this paper. We mainly focus on the preventive control. Here, resorting the solvability aims at calculating the ELSI and apparent power of each line to recognize the weak braches which possibly result in the static voltage instability and/or thermal stability. Honestly, the preventive control probably leads to relatively large control cost when it considers the unsolvable case.

3 Simulation Result

The correctness and effectiveness of the proposed preventive control model is demonstrated using the simulations for the IEEE 30-bus system, IEEE 57-bus system and IEEE 118-bus system. The following assumptions are made to ensure that the three test systems possibly become to loss static voltage stability and/or thermal stability in some contingency conditions.

- In the IEEE 30-bus system, the loads at bus 29 and bus 30 are respectively increased to be 8.8+j3.3 M·VA and 21.2+j3.8 M·VA with an assumption of a constant power factor;
- In the IEEE 57-bus system, the loads at buses 19, 53 and 54 are respectively increased to be 16.5+j3 M·VA, 30+j15 M·VA and 20.5+j7 M·VA with an assumption of a constant power factor.
- In the IEEE 118-bus system, the loads at buses 43, 44 and 45 are respectively increased to be 36+j14M·VA, 62+j31M·VA and 140+j58M·VA with an assumption of a constant power factor.

In order to guarantee power system can respectively satisfy the minimum static voltage stability margin of 15% and 10% in normal operating condition and contingency condition, the threshold α of ELSI is respectively set to be 1.15 and 1.1 in normal operating condition and contingency condition.

3.1 Simulation analysis of the proposed preventive control

Before the proposed preventive control, the information of critical contingencies and corresponding weak branches is shown in Table 1. The transfer capabilities of weak branches, which are shown in the sixth column, are determined according to Equation (3). The calculated results indicate that for the IEEE 30-bus system, the transfer capability of the weak branch 1-2 is its thermal limit in outage of branch 1-3, whereas the transfer capability of the weak branch 29-30 is the static voltage stability limit which is the products of ELSI and actual apparent power in outage of branch 27-29 or 27-30. For the IEEE 57-bus system, the transfer capabilities of weak branches all are determined by the static voltage stability limits. For the IEEE 118-bus system, the transfer capability of the weak branch 43-44 is its thermal limit in outage of branch 44-45; whereas in outage of branch 34-43 or 45-46, the transfer capabilities of the corresponding weak branches are the static voltage stability limit which is the products of ELSI and actual apparent power. It can be seen that the start points for the three test systems are in the insecure operation state since the apparent powers on weak branches in contingency condition exceed their transfer capabilities. Particularly, the IEEE-57 bus system is so near the voltage collapse point following the branch 55-54 outage because the ELSI of the weak branch in this contingency is very close to 1.0.

Table 1. Information of critical contingencies and weak branches before the proposed preventive control

Systems	Critical contingencies / Weak branches	Apparent powers of weak branches(p.u.)	ELSI of weak branches	Thermal limits of weak branches(p.u.)	The transfer capacities of weak branches(p.u.)
IEEE 30-bus system	branch1-3 in outage/ branch1-2	2.8522	3.1385	2.8338	2.8338
	branch27-29 in outage/ branch29-30	0.0980	1.0901	0.2737	0.0971
	branch27-30 in outage/ branch29-30	0.2454	1.0794	0.2737	0.2408
IEEE 57-bus system	branch18-19 in outage/ branch20-19	0.1803	1.0182	0.2688	0.1669
	branch18-19 in outage/ branch21-20	0.2265	1.0229	0.2445	0.2106
	branch29-52 in outage/ branch54-53	0.4310	1.0103	0.4759	0.3958
	branch55-54 in outage/ branch52-53	0.6023	1.0352	0.6708	0.5668
	branch55-54 in outage/ branch54-53	0.2456	1.0006	0.4759	0.2234
IEEE 118-bus system	branch34-43 in outage/ branch43-44	0.4043	1.0607	0.7392	0.3899
	branch44-45 in outage/ branch43-44	0.7789	1.0499	0.7392	0.7392
	branch45-46 in outage/ branch45-49	2.0436	1.0552	2.0712	1.9604

As mentioned in Introduction, in some nonlinear preventive control models, the power flow equality constraints with load parameter and transmission current constraints are respectively used as the static voltage stability constraints and thermal stability constraints, which has limitation when the preventive control considers multi-contingency conditions. Here, the number of static voltage stability and thermal stability constraints in the proposed preventive control model is compared with the static voltage stability constraints and thermal stability constraints mentioned above. The result is shown in Table 2. It can be seen that the number of constraints in the proposed model is far smaller than that of power flow equality constraints with load parameter and transmission current constraints, which can greatly reduce the size of the preventive control problem. This advantage will become more significant for a larger power system.

After the first iteration of the proposed preventive control, the control variables in the base case are adjusted. In the coordinated systems, under the contingency conditions shown in Table1, there are no static voltage stability violation and thermal stability violation on the weak branches indicated in Table 1, which can be seen from Table 3. The Table 3 shows that the ELSI of these branches become larger than the threshold 1.1 and the apparent powers on these branches become lower than their transfer capabilities shown in Table 1.

For the coordinated systems, the ELSI and apparent power of each branch under various contingency conditions are calculated. The result shows that there is no violation on voltage stability and thermal stability. This suggests that the systems become secure from an insecure state through the proposed preventive control model, and the entire

preventive control process for the three test systems ends after the first iteration of preventive control. A few more iterations may be required for other systems. The other results of the entire preventive control for the three test systems are shown in Table4. It can be observed from Table 4 that one iterative process of preventive control is needed for each of the three systems to satisfy all the combined static voltage stability and thermal stability constraints in both the normal operating condition and contingency conditions. The iteration numbers of the PCPDIPM, the active network power losses and load curtailments are also given in Table 4. It can be seen that the load curtailment is not required to ensure the static voltage stability and thermal stability in all contingency conditions for the three test systems with the proposed preventive control.

Table 2. The comparison in the number of static voltage stability constraints and thermal stability constraints

Systems	The number of critical contingencies	The number of weak branches	The number of static voltage stability constraints and thermal stability constraints	
			The number of apparent power constraints in this paper	The number of power flow equality constraints with load parameter and transmission current constraints
IEEE 30-bus system	3	3	9	121
IEEE 57-bus system	3	5	15	342
IEEE 118-bus system	3	3	9	708

Table 3. Information of critical contingencies and weak branches illustrated in Tablelafter the first iteration of the proposed preventive control

Systems	Critical contingencies/ Weak branches	Apparent powers of weak branch (p.u.)	ELSI of weak branch
IEEE 30-bus system	branch1-3 in outage/ branch1-2	2.7961	3.2273
	branch27-29 in outage/ branch29-30	0.0970	1.1681
	branch27-30 in outage/ branch29-30	0.2393	1.1598
IEEE 57-bus system	branch18-19 in outage/ branch20-19	0.1775	1.3193
	branch18-19 in outage/ branch21-20	0.2175	1.5010
	branch29-52 in outage/ branch54-53	0.3791	1.2521
	branch55-54 in outage/ branch52-53	0.5542	1.4918
	branch55-54 in outage/ branch54-53	0.2335	1.2154
IEEE 118-bus system	branch34-43 in outage/ branch43-44	0.3863	1.1405
	branch44-45 in outage/ branch43-44	0.6687	1.3582
	branch45-46 in outage/ branch45-49	1.9257	1.2004

Table 4. Result of the entire preventive control process

Systems	Iteration number of preventive control	Iteration number of PCPDIPM	Network active power loss (p.u.)	Load curtailment (p.u.)
IEEE 30-bus system	1	19	0.1987	0.0000
IEEE 57-bus system	1	18	0.2737	0.0000
IEEE 118-bus system	1	13	1.3565	0.0000

3.2 Validating the static voltage stability after the proposed preventive control

A further simulation analysis using the continuation power flow (CPF) method is carried out to validate the correctness and effectiveness of the proposed preventive control. Due to limitation of space, only one contingency case for the IEEE 30-bus system, which is the outage of branch 27-30, is illustrated.

The PV curves at bus 30 after the outage of branch 27-30, which is for the two cases without and with the proposal preventive control, are plotted in Fig.2. In the CPF method, the load parameter λ, which represents the distance from the current operating point to the voltage collapse point, is defined as voltage stability margin [8, 14]. The system is assumed to be voltage secure if this margin is greater than a specifically required value which generally is 0.1 in a contingency condition [8, 14]. In this example, "λ=0" denotes the operating point right after the outage of branch 27-30. Point A and point B respectively denote the operating points following the contingency without and with the proposed preventive control. Without the proposed preventive control, the critical value of load parameter λ is 0.0794 following the outage of branch 27-30, which cannot satisfy the desired margin of 0.1 in the contingency condition. Also, the voltage magnitude of bus 30 at the point A is lower than 0.85 p.u. and is not allowed in real power system operation. With the proposed preventive control, on the other hand, the critical value of load parameter λ is increased to be 0.1609 which meets the requirement of the desired static voltage stability margin in the contingency condition, and the voltage magnitude of bus 30 at the point B becomes higher than 0.9 p.u. and is acceptable in actual real power system. The results in Figure2 verified that the proposed preventive control model could correctly and effectively bring the system from an insecure state to a secure state.

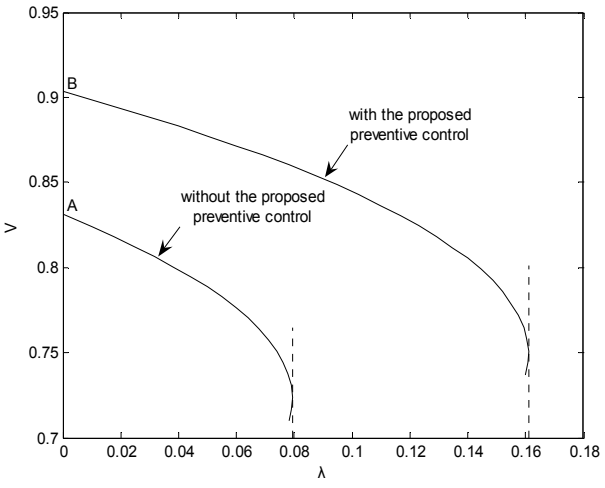

Fig . 2. PV curves at bus 30 after the outage of branch 27-30

4 Conclusion

This paper proposed a new preventive control optimal model for both static voltage stability and thermal stability. And the proposed model has the following three features. Firstly, the proposed model can reflect the nonlinear characteristics of power system and overcome the limitations of linearization models. Secondly, the static voltage stability and thermal stability constraints are represented by the apparent power constraints on weak branches which can be easily identified by a local voltage stability index. This can greatly reduce the number of preventive control constraints since the number of weak branches causing thermal instability and/or voltage instability is always small in a real power system. Thirdly, the proposed model is expressed in a purely quadratic form which can be efficiently solved using the predictor-corrector primal dual interior method. The second and third features together can significantly reduce computational efforts.

The IEEE 30-bus system, IEEE 57-bus system and IEEE 118-bus system are used as examples. The correctness and effectiveness of the proposed preventive control model are demonstrated by the simulation results of the three test systems and verified by the results obtained from the continuation power flow method.

It should be pointed out that the proposed preventive control applies to the static voltage stability and thermal stability problem, rather than voltage instability and thermal instability caused by the dynamic problem of the system.

5 List of Symbols

b_{ij} actual susceptance of weak branch ij
b_{i0} susceptance between the ground and bus i
S' inverse matrix of coefficient matrix B' in the PQ decoupled method
S'' inverse matrix of coefficient matrix B'' in the PQ decoupled method
N_B number of buses
N_G number of generators
N_C number of shunt capacitors
N_R number of shunt reactors
N_T number of loading tap changers (LTC)
S_{Li} set of line branches or un-load tap changers connected to bus i
S_{Ti} set of LTC branches connected to bus i
S_{L_weak} weak branch set
P_{Di} active power load at bus i
Q_{Di} reactive power load at bus i
C_i active power load curtailment at bus i
P_{Gi} active power output of generator i
Q_{Gi} reactive power output of generator i
Q_{Ci} reactive power injection of shunt capacitor i
Q_{Ri} reactive power injection of shunt reactor i
k_t turn ratio of tth LTC
e_i real part of voltage at bus i

f_i imaginary part of voltage at bus i
U_i amplitude of voltage at bus i
α threshold value of ELSI

Acknowledgement
This work was supported in part by the National Natural Science Foundation of China under Contract (51007098) and Scientific Research Foundation of State Key Lab. of Power Transmission Equipment and System Security (2007DA10512710201).

References:

[1]C.W.Taylor, *Power system voltage stability*, first ed., McGraw-Hill. Inc., 1994.

[2]T.Van Custem, and C.Vournas, *Voltage stability of electric power systems*, Kluwer Academic Publishers, 1998.

[3]P.Kunder, *Power system stability and control*, McGraw-Hill. Inc., 1994.

[4]B.Yang, V.Vittal, and G.T.Heydt, Slow- coherency -based controlled islanding-a demonstration of the approach on the August 14, 2003 blackout scenario, *IEEE Transactions on Power Systems*, Vol.21, No. 4, 2006, pp. 1840- 1847.

[5]J.Martinez-Crespo, J.Usaola, and J.L.Fernandez, Security-constrained optimal generation scheduling in large-scale power systems, *IEEE Transactions on Power Systems*, Vol.21, No. 1, 2006, pp.321-332.

[6]L.Lenoir, I. Kamwa, and L.-A. Dessaint, Overload alleviation with preventive-corrective static security using fuzzy logic, *IEEE Transactions on Power Systems*, Vol.24, No.1, 2009, pp.134-145.

[7]E.Lobato, L.Rouco, T.Gómez, et al, Preventive analysis and solution of overloads in the Spanish electricity market, *Electric Power Systems Research* Vol.68, 2004, pp. 185-192.

[8]Z.H.Feng, V.Ajjarapu, and D.J.Maratukulam, A comprehensive approach for preventive and corrective control to mitigate voltage collapse, *IEEE Transactions on Power Systems*, Vol.15, No.2, 2000, pp.791-797.

[9]F.Capitanescu, and T.Van Cunstem, Preventive control of voltage security margins: a multi-contingency sensitivity-based approach, *IEEE Transactions on Power Systems*, Vol.17, No.2. 2002, pp. 358-364.

[10]J.Q.Zhao, B.M. Zhang, and H. D. Chiang, An optimal power flow model and approach with static voltage stability constraints, *IEEE/PES Transmission and Distribution Conference and Exhibition*, 2005, pp. 1-6.

[11]Y.Fu, M.Shahidehpour,and Z.Li, AC contingency dispatch based on security- constrained unit commitment, *IEEE Transactions on Power Systems* Vol.21, No.2, 2006, pp.897-908.

[12]E.Lobato, L.Rouco, T. Gómez, et al , A practical approach to solve power system constraints with application to the Spanish electricity market, *IEEE Transactions on Power Systems*, Vol.19, No.4, 2004, pp.2029-2037.

[13]X.Fu,and X.F.Wang, A unified preventive control approach considering voltage instability and thermal overload, *IET Generation, Transmission & Distribution*,Vol.1, No.6, 2007, pp.864-871.

[14]A.J.Conejo, F.Milano, and R.García-Bertrand, Congestion management ensuring voltage stability. *IEEE Transactions on Power Systems*, Vol.21, No.2, 2006, pp.357-364.

[15]X.S.Zhou, X.J.Luo, and Z.W.Peng, Congestion management ensuring voltage stability under multicontingency with preventive and corrective controls, *IEEE Power and Energy Society General Meeting-Conversion and Delivery of Electric Energy in the 21st Century*, 2008, pp. 1-8.

[16]Q.Wang, and V.Ajjarapu, A critical review on preventive and corrective control against voltage collapse, *Electric Power Components and Systems*, Vol.12, No.29, 2001, pp. 1133-1144.

[17]F.Capitanescu, M.Glavic, D.Ernst, et al, Contingency filtering techniques for preventive security- constrained optimal power flow, *IEEE Transactions on Power Systems* , Vol.22, No.4, 2007, pp.1690-1697.

[18]M.Moghavvemi, and M.O.Faruque, Power system security and voltage collapse: a line outage based indicator for prediction, *Electrical Power and Energy Systems*, Vol.21,1999, pp. 455-461.

[19]B.Venkatesh, R. Ranjan, and H.B. Gooi, Optimal reconfiguration of radial distribution systems to maximize loadability, *IEEE Transactions on Power Systems*, Vol.19, No.1, 2004, pp.260-266.

[20]W.Y. Li, J.Yu, Y.Wang, et al, *Method and system for real time identification of voltage stability via identification of weakest lines and buses contributing to power system collapse*, U.S. Patent 7816927, Oct. 2010 (filed Jul. 27, 2007), China Patent Zl 200710092710.1, Aug. 2009 (filed Sep. 17, 2007).

[21]W.Yan, J.Yu, D.C.Yu, et al, A new optimal reactive power flow model in rectangular form and its solution by predictor corrector primal dual interior point method, *IEEE Transactions on Power Systems*, Vol.21, No.1, 2006, pp.61-67.

[22]S. Granville, J. C. O. Mello, and A. G. C. Melo, Application of interior point methods to power flow unsolvability, *IEEE Transactions on Power Systems*, Vol.11, No.2, 1996, pp.1096-1103.

[23]K.R.C.Mamandur, and G.J.Berg, Efficient simulation of line and transformer outage in power system, *IEEE Transactions on Power Systems*, PAS-101, No.10, 1982, pp.3733-3741.

Appendix:

Using the static security analysis based on the PQ decoupled method, the active power increment ΔP_k, ΔP_l and reactive power increment ΔQ_k, ΔQ_l at bus k and bus l in the contingency state of branch kl outage can be calculated by Equations (A.1) and (A.2).

$$\begin{bmatrix}\Delta P_k\\ \Delta P_l\end{bmatrix}=\begin{bmatrix}a_{11} & a_{12}\\ a_{21} & a_{22}\end{bmatrix}\begin{bmatrix}P_{kl0}(e,f)\\ P_{lk0}(e,f)\end{bmatrix} \quad (A.1)$$

$$\begin{bmatrix}\Delta Q_k\\ \Delta Q_l\end{bmatrix}=\begin{bmatrix}c_{11} & c_{12}\\ c_{21} & c_{22}\end{bmatrix}\begin{bmatrix}Q_{kl0}(e,f)\\ Q_{lk0}(e,f)\end{bmatrix} \quad (A.2)$$

where

$$\begin{bmatrix}a_{11} & a_{12}\\ a_{21} & a_{22}\end{bmatrix}=\left(\begin{bmatrix}1 & 0\\ 0 & 1\end{bmatrix}-\begin{bmatrix}-b_{kl} & b_{kl}\\ b_{kl} & -b_{kl}\end{bmatrix}\begin{bmatrix}S'_{kk} & S'_{kl}\\ S'_{lk} & S'_{ll}\end{bmatrix}\right)^{-1} \quad (A.3)$$

$$\begin{bmatrix}c_{11} & c_{12}\\ c_{21} & c_{22}\end{bmatrix}=\left(\begin{bmatrix}1 & 0\\ 0 & 1\end{bmatrix}-\begin{bmatrix}-(b_{kl}+2b_{k0}) & b_{kl}\\ b_{kl} & -(b_{kl}+2b_{k0})\end{bmatrix}\begin{bmatrix}S''_{kk} & S''_{kl}\\ S''_{lk} & S''_{ll}\end{bmatrix}\right)^{-1} \quad (A.4)$$

where, b_{kl} represents the susceptance of outage branch kl; b_{k0} or b_{l0} represents the susceptance between the ground and bus k or bus l.

For the weak branch ij, the voltage angle increment $\Delta\theta_i, \Delta\theta_j$ and the voltage magnitude increment $\Delta U_i, \Delta U_j$ at bus i and bus j can be calculated by Equations (A.5) and (A.6).

$$\begin{bmatrix}\Delta\theta_i\\ \Delta\theta_j\end{bmatrix}=\begin{bmatrix}S'_{ik} & S'_{il}\\ S'_{jk} & S'_{jl}\end{bmatrix}\begin{bmatrix}\Delta P_k\\ \Delta P_l\end{bmatrix} \quad (A.5)$$

$$\begin{bmatrix}\Delta U_i\\ \Delta U_j\end{bmatrix}=\begin{bmatrix}S''_{ik} & S''_{il}\\ S''_{jk} & S''_{jl}\end{bmatrix}\begin{bmatrix}\Delta Q_k\\ \Delta Q_l\end{bmatrix} \quad (A.6)$$

Using Equations (A.5) and (A.6), the active power increment ΔP_{ij} (e, f)and the reactive power increment ΔQ_{ij} (e, f)of weak branch ij in the contingency state of branch kl in outagecan be calculated by Equations (A.7) and (A.8).

$$\Delta P_{ij}(e,f)=\begin{bmatrix}-b_{ij} & b_{ij}\end{bmatrix}\begin{bmatrix}\Delta\theta_i\\ \Delta\theta_j\end{bmatrix} \quad (A.7)$$

$$\Delta Q_{ij}(e,f)=\begin{bmatrix}-(b_{ij}+2b_{i0} & b_{ij}\end{bmatrix}\begin{bmatrix}\Delta U_i\\ \Delta U_j\end{bmatrix} \quad (A.8)$$

Combining Equations (A.1)-(A.8), Equations (7) and (8) can be obtained.